

## Observation of Two Andreev-Like Energy Scales in $\text{La}_{2-x}\text{Sr}_x\text{CuO}_4$ Superconductor–Normal-Metal–Superconductor Junctions

G. Koren\* and T. Kirzhner

*Physics Department, Technion - Israel Institute of Technology Haifa, 32000, Israel*

(Received 19 August 2010; published 5 January 2011)

Conductance spectra measurements of highly transparent junctions made of superconducting  $\text{La}_{2-x}\text{Sr}_x\text{CuO}_4$  electrodes and a nonsuperconducting  $\text{La}_{1.65}\text{Sr}_{0.35}\text{CuO}_4$  barrier are reported. At low temperatures below  $T_c$ , these junctions have two prominent Andreev-like conductance peaks with clear steps at energies  $\Delta_1$  and  $\Delta_2$  with  $\Delta_2 > 2\Delta_1$ . No such peaks appear above  $T_c$ . The doping dependence at 2 K shows that both  $\Delta_1$  and  $\Delta_2$  scale roughly as  $T_c$ .  $\Delta_1$  is identified as the superconducting energy gap, while a few scenarios are proposed as for the origin of  $\Delta_2$ .

DOI: 10.1103/PhysRevLett.106.017002

PACS numbers: 74.25.F-, 74.25.Dw, 74.45.+c, 74.72.-h

The issue of two distinct energy gaps in the cuprates has been discussed by many authors, and the question whether both are related to superconductivity is still controversial [1–4]. In one scenario, one energy gap is the coherence gap which opens at  $T_c$  with the onset of phase coherent superconductivity, while the other gap opens at  $T^*$  which marks the crossover to the pseudogap regime and possibly the creation of uncorrelated pairs [5]. In contrast to this scenario, some angle-resolved photoemission spectroscopy (ARPES) measurements show only a single energy gap, which indicate that the superconducting gap and the pseudogap might be the same entity [6,7]. In another scenario, the regime above  $T_c$  in the underdoped cuprates which exhibits a signature of the condensate, can be attributed to strong superconducting fluctuations. This behavior was found in measurements of the Nernst effect [8], whose  $T_c$  (onset) values scale with doping roughly as the superconducting dome. This effect, therefore, is related to  $T_c$  and apparently depends on more than one energy scale of the condensate. Previous point contact measurements of tunneling and Andreev conductance have shown that the tunneling gap which scales as  $T^*$  is larger than the Andreev gap which follows  $T_c$  [2,9–11]. In the present study we report on similar conductance measurements in ramp-type junctions of the  $\text{La}_{2-x}\text{Sr}_x\text{CuO}_4$  (LSCO $x$  or LSCO) system, but due to their high transparency we observe mostly Andreev gaps. Surprisingly, we find two different such gaps in this system below  $T_c$  both of which scale versus doping roughly as the superconducting dome. Only single gaps were observed in previous conductance measurements in LSCO $x$  [10–13]. The results though show that in Refs. [10–12] the gaps follow  $T_c$  while in Ref. [13] the gaps scale as  $T^*$ . The present low energy Andreev peak in the conductance spectra is attributed to the superconducting gap, while a few scenarios are discussed in relation to the origin of the second high energy feature in the spectra.

Highly transparent superconductor–normal-metal–superconductor (S-N-S) junctions of the cuprates can be obtained if the  $S$  electrodes and the  $N$  barrier have similar

density of states and Fermi velocities. In the LSCO system the doping levels are determined mostly by the Sr content, provided the same oxygen annealing process is used. Therefore, highly transparent junctions can be realized, if the  $S$  electrodes are in the superconducting regime ( $0.06 \leq x \leq 0.25$ ) while the  $N$  barrier is nonsuperconducting with  $x \approx 0.35$ – $0.45$ . We thus investigated LSCO $x$ -LSCO35-LSCO $x$  ramp-type junctions with  $x$  values of 0.1, 0.125, 0.15 and 0.18, in order to determine the various Andreev-like gaps and study the doping dependence (or phase diagram) of these gaps. Ten junctions were prepared for each doping level along the antinode direction in the geometry shown in the inset to Fig. 1, on  $1 \times 1 \text{ cm}^2$  wafers of (100)  $\text{SrTiO}_3$  (STO). All the different LSCO layers were grown epitaxially with the  $c$  axis normal to the wafer, and thus  $a$ - $b$  plane coupling was obtained between the base and cover electrodes. All junctions had the same geometry with  $5 \mu\text{m}$  width, and 77 and 33 nm films and barrier thicknesses, respectively. Typical four-probe results of the resistance versus temperature for  $x = 0.1$

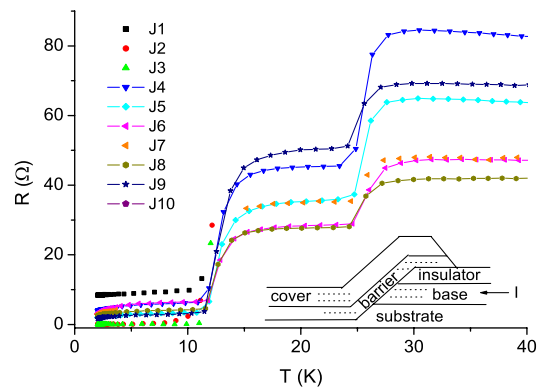


FIG. 1 (color online). Resistance versus temperature of all the LSCO10 junctions on the wafer. The inset shows a schematic drawing of a ramp-type junction, where the 77 nm thick base and cover electrodes are made of LSCO $x$  and the 33 nm thick barrier is made of LSCO35.

are shown in Fig. 1. One can easily see the two distinct transition temperature onsets at 28 and 15 K, which correspond to the  $T_c$  values of the cover and base electrodes, respectively. The reason for this is that the base electrode on the pristine STO surface is more strained than the cover electrode which is grown on a 33 nm thick LSCO35 layer on top of the ion milled area of the STO wafer [14]. Below about 10 K, the quite constant junctions' resistance can be seen which ranges between 0–8  $\Omega$ .

Figure 2 shows a representative normalized conductance spectrum at 2 K of the junction J4 of Fig. 1. This spectrum has three pronounced features. The first is a narrow zero bias conductance peak (ZBCP), the second is a domelike peak of intermediate width which is superimposed on a third feature which is even broader. The conductance data is therefore the result of a sum of three components which can be written as  $G(\text{total}) = G(\Delta_0) + G(\Delta_1) + G(\Delta_2)$ . Note that the gap feature in the S-N-S junction always appears at  $2\Delta$  [15]. Interference phenomena such as Tomasch [16] or McMillan-Rowel [17] oscillations do not affect this gap voltage and are absent in the present study, though they had been observed previously in similar  $\text{YBa}_2\text{Cu}_3\text{O}_{7-\delta}$  based S-N-S junctions [18]. Furthermore, the use of S-N junctions with a single interface involves significant leads' resistance [19]. We therefore decided to work with S-N-S junctions with possible interference effects but with zero lead resistance and accurate energy or voltage scale. We used the Blonder, Tinkham, and Klapwijk (BTK) model modified for a  $d$ -wave superconductor given by Tanaka and Kashiwaya to fit our data [20]. The three conductance components  $G(\Delta_i)$  of these fits are shown in Fig. 2 together with the total conductance curve  $G(\text{total})$  which fits the data quite well. The barrier strength  $Z_i$ , the Andreev gap parameters  $\Delta_i$  and the lifetime broadening  $\Gamma_i$  are also given in Fig. 2. One can see that the  $Z_i$  values are quite low which indicates a highly transparent

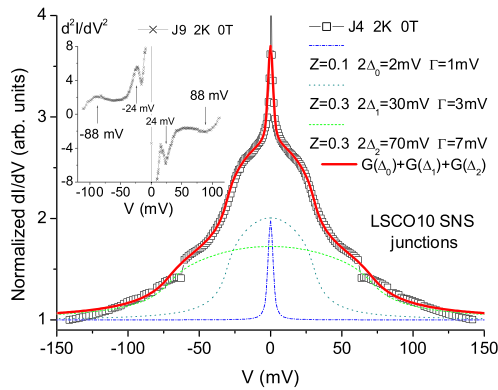


FIG. 2 (color online). Conductance spectrum of an antinode S-N-S junction of LSCO10-LSCO35-LSCO10 at 2 K with a fit to the BTK model for a  $d$ -wave superconductor. The three components of the fit with  $\Delta_0$ ,  $\Delta_1$  and  $\Delta_2$  are also shown. The inset shows the derivative of the conductance data of another junction on the same wafer.

junction. This justifies our use of the antinode direction formula without mixing of the node direction, since both are quite similar when the  $Z_i$  values are small. We also note that the maximum conductance value of each component in Fig. 2 is at around 2 which is like the expected Andreev value of the conductance of a pair for each incident electron. Although this fitting procedure involves many parameters, the clear Andreev-like gap features at  $\Delta_1$  and  $\Delta_2$  can be deduced from the raw data directly by taking the derivative of the conductance as shown in the inset. This was done for a different junction on the same wafer, and one can see that the peak locations are quite close to the different  $2\Delta_i$  obtained before, but this also reflects the spread of these values on the same wafer. Additional conductance spectra that show the spread of the  $2\Delta_i$  values are shown in Figs. 4S, 5S and 6S of the supplementary material for LCO15-LSCO35-LSCO15 junctions [19]. Fig. 3S there shows that the conductance spectra of LSCO10-LSCO35 S-N junctions [19] are basically quite similar to the results of Fig. 2 here on S-N-S junctions. We note in passing that the sharp resonances at  $\pm 62$  mV in Fig. 2 are not very common and appear in about one out of ten junctions on a wafer.

A typical conductance spectrum of a LSCO18-LSCO35-LSCO18 junction at 2 K together with a fit and its three components as before are shown in Fig. 3. The dominant component contributing to this spectrum is the highly transparent one at  $\Delta_1$ , but unlike in Fig. 2, its maximum value now is above 10 and not around 2. We attribute this behavior to the presence of bound states which can cause this effect [20]. The  $\Delta_2$  feature is still quite clear but has a small spectral weight as compared to that of  $\Delta_1$ . It also has a lower transparency and shows a tunnelinglike behavior. The third feature near zero bias now looks like a split ZBCP, again with intermediate transparency and tunnelinglike behavior. The very narrow ZBCP of Fig. 2 is gone, and only a remnant critical current is observed. The  $d^2I/dV^2$  of

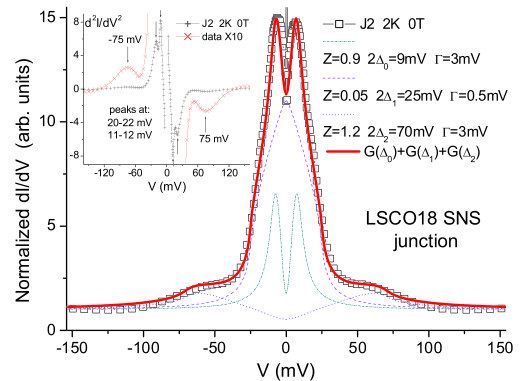


FIG. 3 (color online). Conductance spectrum of an antinode junction of LSCO18-LSCO35-LSCO18 at 2 K with a fit to the  $d$ -wave BTK model together with the three components of this fit with  $\Delta_0$ ,  $\Delta_1$ , and  $\Delta_2$ . The inset shows the derivative of the conductance data of the main panel.

the same junction (inset) show that the peak energies now are even closer to the fit in comparison to the results of Fig. 2. Figure 4 shows a few conductance spectra of the same junction at different temperatures. As expected, both  $\Delta_1$  and  $\Delta_2$  are suppressed with increasing temperature while  $\Delta_0$  is basically unaffected. The inset to Fig. 4(b) shows that  $\Delta_2(T)$  behaves quite similarly to a BCS gap versus temperature, and therefore can be considered as a gaplike feature in the density of states. In addition, we found that in all junctions above  $T_c$  of both electrodes at about 30 K, all the conductance spectra were flat (not shown), which indicates that no Andreev scattering could be observed. This is in agreement with a previous finding by Dagan *et al.* in normal-metal–insulator–superconductor junctions [21]. Above  $T_c$  however, the junction contribution to the conductance is quite small compared to the significant leads' resistance, and any change due to possible pairing in the pseudogap regime might be too small to be observed. Conductance spectra were also measured under magnetic fields of up to 6 T (not shown), and already at 2 T a strong suppression of all the gaplike features was observed. We thus conclude that both  $\Delta_1$  and  $\Delta_2$  represent gaplike features of the LSCO $_x$  system.

Figure 5 summarizes on the phase diagram of LSCO the  $\Delta_1$  and  $\Delta_2$  results of the present study at 2 K versus doping.

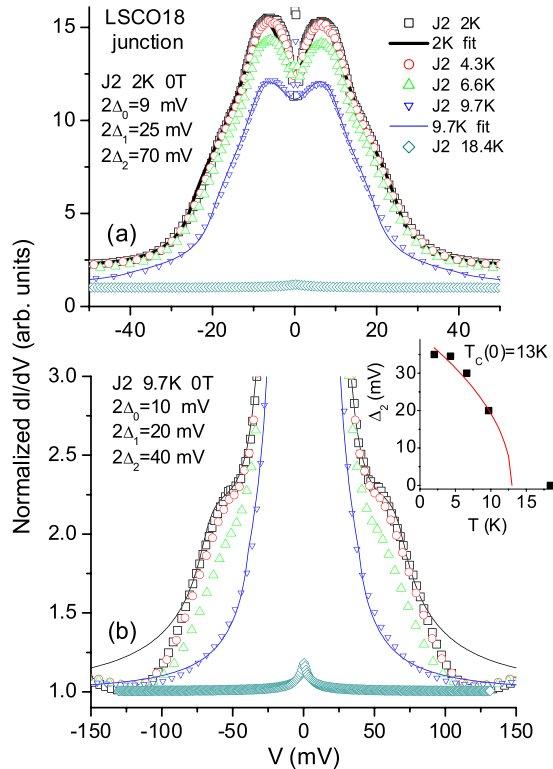


FIG. 4 (color online). Conductance spectra of the same junction as in Fig. 3 at various temperatures  $T$  at low bias (a), and up to high bias with zooming up on low conductances (b). The inset to (b) shows the large gap  $\Delta_2$  behavior versus  $T$  (squares) with a  $\Delta_2(0)\sqrt{(T_c - T)/T_c}$  fit (line).

Also shown are STM [12] and ARPES gaps [4,22,23], and the  $T_c$  values of film and bulk LSCO [24]. The  $\Delta_i$  values represent mean values of all working junctions on the wafer for each doping level and their statistical error. One can see that the general doping dependence of both  $\Delta_1$  and  $\Delta_2$  follows roughly the superconducting dome. The  $\Delta_2$  value at optimal doping of  $x = 0.15$  is strongly enhanced by a factor of about two compared to the  $\Delta_2$  values at the 0.1 and 0.18 doping levels. The  $\Delta_1$  value is strongly suppressed at the  $x = 1/8$  doping level, similar to  $T_c$ . The  $\Delta_1$  results agree with the STM observations [12], while the previous point contact results with  $\Delta \approx 6-8$  meV [9–11] are found on the lower side of the  $\Delta_1$  values. Different ARPES gaps for LSCO $_x$  were found by different groups at  $x = 0.145$  and 0.15 doping levels. Shi *et al.* have measured  $\Delta = 14$  and 16 meV well below and well above  $T_c$ , respectively [23], while the corresponding gaps that Therashima *et al.* [22] have measured were  $\Delta = 34$  and 37 meV. The former agree with our  $\Delta_1 = 19 \pm 3$  meV value at  $x = 0.15$  which also agrees with Yoshida *et al.* who measured  $\Delta_0 \approx 20$  meV [4], but the latter as well as the ARPES gap of about 25 meV at  $x = 0.105$ , fall in between the present  $\Delta_1$  and  $\Delta_2$  values. Our results thus seem to suggest that  $\Delta_1$  is the superconducting gap. Its low value at 1/8 doping also supports this conclusion if stripes are taken into account [5,25].  $\Delta_2$  seems to be related to  $T_c$ , since it roughly follows its doping dependence, but its origin is not so straightforward and different scenarios for it will be discussed next.

First, since the  $\Delta_2$  feature in the conductance spectra is quite small, it might be attributed to a background “step down” in the highly transparent junctions due to any excitation mode with energy  $\hbar\omega$  which will appear at  $eV = \hbar\omega - \Delta_1$  as discussed by Kirtley [26]. This result was obtained using a theory of inelastic transport at the junction’s interface, where the  $\hbar\omega$  excitations by tunneling or Andreev processes can be due to holons, bosons, phonons, and so on [9,27]. This gives symmetric spectra

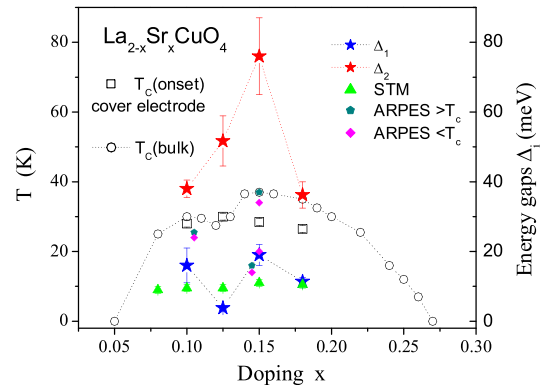


FIG. 5 (color online). The phase diagram of all the LSCO $_x$  junctions versus doping  $x$ . Shown are the bulk and cover electrode film transition temperatures, the two Andreev-like energy gaps  $\Delta_1$  and  $\Delta_2$  of the present study at 2 K, and previous STM gaps at 4.2 K [12] and ARPES gaps [4,22,23].

in agreement with the present results, but the doping dependence of  $\Delta_2$  implies that these excitations have to be related to superconductivity and the way they actually do needs further theoretical treatment. A second scenario for  $\Delta_2$  is that it might be related to the Van Hove singularity (VHS) in the 2D LSCO system. Using the  $tt'J$  model it was shown that in addition to the coherence peaks at the gap energy  $\Delta$ , two new and symmetric peaks appear at 2–3 times  $\Delta$  in the conductance spectra due to the VHS [28]. This agrees with the present symmetric spectra and the values of  $\Delta_2$ . However, when a  $tt't''J$  model was used [29], asymmetric spectra were obtained which disagree with our results but nevertheless, the peak energies are still of the order of  $\Delta_2$ . The doping dependence that follows from these results shows a monotonous increase of the energy due to the VHS feature with decreased doping, similar to the doping dependence of the pseudogap. This is in clear contradiction to our results, but in view of the fact that the calculations involved were done in attempt to explain the asymmetrical tunneling spectra of BSCO [29–31], one cannot rule out that further theoretical analysis for LSCO might yield different results. Finally, although we are puzzled by the possible existence of a proper Andreev gap at such high energies as  $\Delta_2$ , the reasonably good fits to our data using the  $d$ -wave BTK model [20], might indicate that  $\Delta_2$  is originated in such a gap in the density of states. To relate this to superconductivity as observed in Fig. 5, one would need pairs with an even larger condensation energy. In this scenario then,  $\Delta_2$  will be related to  $\Delta_1$ , but their relation to  $T_c$  will involve different doping dependent functions that will have to account for the fact that  $\Delta_1(x = 0.15)/\Delta_1(x = 0.1) \sim 1$  while  $\Delta_2(x = 0.15)/\Delta_2(x = 0.1) \sim 2$ . Clearly, a thorough theoretical modeling as for the origin of  $\Delta_2$  is needed, and this might add to our understanding of the high temperature superconductors.

In conclusion, two Andreev-like energy gaps have been observed in the LSCO $x$  cuprates, both of which scale roughly with  $T_c$  versus doping.  $\Delta_1$  is identified as the superconducting energy gap, while the origin of  $\Delta_2$  which is also related to superconductivity, is unclear at the present time and needs further theoretical modeling.

This research was supported in part by the Israel Science Foundation, the joint German-Israeli DIP project and the Karl Stoll Chair program in advanced materials at the Technion.

- \*gkoren@physics.technion.ac.il; <http://physics.technion.ac.il/~gkoren>
- [1] Ch. Renner *et al.*, *Phys. Rev. Lett.* **80**, 149 (1998).
  - [2] G. Deutscher, *Nature (London)* **397**, 410 (1999).
  - [3] W. S. Lee *et al.*, *Nature (London)* **450**, 81 (2007).
  - [4] T. Yoshida *et al.*, *Phys. Rev. Lett.* **103**, 037004 (2009).
  - [5] V. J. Emery and S. A. Kivelson, *Nature (London)* **374**, 434 (1995).
  - [6] A. Kanigel *et al.*, *Phys. Rev. Lett.* **101**, 137002 (2008).
  - [7] U. Chatterjee *et al.*, *Nature Phys.* **6**, 99 (2009).
  - [8] Yayu Wang, L. Li, and N. P. Ong, *Phys. Rev. B* **73**, 024510 (2006).
  - [9] G. Deutscher, *Rev. Mod. Phys.* **77**, 109 (2005).
  - [10] G. Deutscher *et al.*, *Physica (Amsterdam)* **282–287C**, 140 (1997).
  - [11] R. S. Gonnelli *et al.*, *Eur. Phys. J. B* **22**, 411 (2001).
  - [12] O. Yuli *et al.*, *Phys. Rev. B* **75**, 184521 (2007).
  - [13] M. Oda *et al.*, *Supercond. Sci. Technol.* **13**, R139 (2000).
  - [14] J. P. Locquet *et al.*, *Nature (London)* **394**, 453 (1998).
  - [15] M. Tinkham, *Introduction to Superconductivity* (McGraw-Hill, New York, 1996), pp. 77.
  - [16] W. J. Tomasch, *Phys. Rev. Lett.* **15**, 672 (1965).
  - [17] J. M. Rowell *et al.*, *Phys. Rev. Lett.* **16**, 453 (1966).
  - [18] O. Neshet and G. Koren, *Phys. Rev. B* **60**, 9287 (1999); **60**, 14893 (1999); *Appl. Phys. Lett.* **74**, 3392 (1999).
  - [19] See supplementary material at <http://link.aps.org/supplemental/10.1103/PhysRevLett.106.017002> for additional conductance spectra of S-N and S-N-S junctions of the LSCO $x$ -LSCO35 system.
  - [20] G. E. Blonder, M. Tinkham, and T. M. Klapwijk, *Phys. Rev. B* **25**, 4515 (1982); Y. Tanaka and S. Kashiwaya, *Phys. Rev. B* **53**, 9371 (1996).
  - [21] Y. Dagan *et al.*, *Phys. Rev. B* **61**, 7012 (2000).
  - [22] K. Terashima *et al.*, *Phys. Rev. Lett.* **99**, 017003 (2007).
  - [23] M. Shi *et al.*, *Phys. Rev. Lett.* **101**, 047002 (2008).
  - [24] T. Matsuzaki *et al.*, *J. Phys. Chem. Solids* **62**, 29 (2001).
  - [25] H. Sato *et al.*, *Physica (Amsterdam)* **408–410C**, 848 (2004).
  - [26] J. R. Kirtley, *Phys. Rev. B* **47**, 11379 (1993).
  - [27] P. W. Anderson and Z. Zou, *Phys. Rev. Lett.* **60**, 132 (1988).
  - [28] A. J. Fedro and D. D. Koelling, *Phys. Rev. B* **47**, 14342 (1993).
  - [29] B. W. Hoogenboom *et al.*, *Phys. Rev. B* **67**, 224502 (2003).
  - [30] T. C. Ribeiro and X. G. Wen, *Phys. Rev. Lett.* **97**, 057003 (2006).
  - [31] G. L. de Castro *et al.*, *Phys. Rev. Lett.* **101**, 267004 (2008).